Japanese Journal of Applied Physics
Vol. 43, No. 5B, 2004, pp. L665–L668

Theoretically Predicted Nonlinear Phase Imbalance Requirement for Delayed-Interference Signal-Wavelength Convertors (DISC)

Yoshiyasu UENO*

Graduate School of Electronic Engineering, University of Electro-Communications, 1-5-1 Chofugaoka, Chofu, Tokyo 182-8585, Japan

(Received November 12, 2003; accepted April 1, 2004; published April 28, 2004)

We have studied the previously demonstrated wavelength conversion of 168-Gb/s random data pulses with semiconductor-optical-amplifier (SOA)-based delayed-interference signal-wavelength converters (DISC). Consequently, we predict an additional requirement for the converters — the nonlinear phase shifts in the two-split interference components must be unbalanced. [DOI: 10.1143/JJAP.43.L665]

KEYWORDS: wavelength conversion, delayed-interference signal-wavelength converter (DISC), semiconductor optical amplifier (SOA), nonlinear phase shift, imbalance, theoretical model, pseudorandom signal, relaxation, Mach-Zehnder interferometer, calcite

Ultrafast wavelength conversion of either clock pulses or random data pulses has been successfully demonstrated in a frequency range from 40 to 160 GHz[1–8] using delayed-interference wavelength convertors (DISC).[9] The wavelength conversion of 168-GHz clock pulses[2] and that of 168-Gb/s randam-data pulses[5] have been the record-high-frequency all-optical-gating demonstration with semiconductor-material-based *all-optical* gates to date, to the authors' best knowlege. In ref. 5, error-free wavelength conversion of 168-Gb/s random data pulses has successfully been demonstrated. Relatively large noise existed, however, in the eye diagram of the 10.5-Gb/s demultiplexed signal (in Fig. 3 of ref. 5) that was observed with a 30-GHz sampling scope after the 168-Gb/s wavelength conversion and the 16:1 all-optical demultiplexing. A relatively large power penalty of 6 dB was also reported from the error rate measurement of the 10.5-Gb/s demultiplexed signals. The origin of the noise and the power penalty has not been indentified, in the present authors' knowledge. In this work, we have studied the validity of the concept of the pseudorandom DISC wavelength conversion and found an additional operating condition. Consequently we speculate that this condition would have only partially been fullfilled in the previously-reported 168-Gb/s wavelength conversion.

According to the original concept that was proposed in refs. 1, 3, and 9 by the present author and his coworkers, the DISC scheme consists of a semiconductor optical amplifier (SOA) and an asymmetric Mach-Zehnder interferometer (AMZI) as is schematically depicted in Fig. 1(a). Each time an input pulse with a wavelength λ_1 is amplified by the SOA, the co-propagating continuous-wave (CW) light is cross-phase-modulated as well as cross-gain-modulated. When the modulated CW light with a wavelength λ_2 passes through the AMZI, wavelength-converted pulses with the wavelength λ_2 are generated at the interferometer's output. The delay time Δt between the two-split modulated CW light effectively determines the width of the all-optical gating window and consequently the width of the converted pulses. The carrier-recovery-induced slow components in the two-split CW light are cancelled by each other in a manner similar to the mechanism of a Symmetric Mach-Zehnder switch.[10]

The experimental setup for realizing the DISC scheme in the previous works[1–3,5,7,9] is schematically shown in Fig. 1(b). In fact the AMZI's were built with quarter-waveplates (Q), half-waveplates (H), a birefringent crystal, an optical phase retarder (R), and a polarizer (P). A polarization-insensitve bulk-active-layer SOA was used. A linearly-polarized CW light had been supposed to be input to the SOA, and to be cross-gain-modulated and cross-phase-modulated in the SOA by the co-propagating pulses. The linear polarization had been supposed to be approximately maintained at the SOA output, because of its polarization insensitivity. After the CW light is modulated inside the SOA, the CW light had been supposed to be split into two orthogonally polarized components (A and B) inside the calcite crystal block, whose optical axis is set in its facet planes. Because of the strong birefringence of the crystal, the one polarized component B is delayed by a specific time Δt, with respect to the other component A. The optical phase bias between the two components is adjusted with an optical phase retarder whose optical axis is set parallel to that of the calcite. The polarizer in Fig. 1(b) is regarded as the interferometer output in Fig. 1(a). It should be noted that all of the waveplate angles, the optical phase bias, and the polarizer angle in the previous experiment had phenomenologically been optimized with monitoring the wavelength-converted random signal waveform.[5,7]

According to the original concept described in refs. 1, 3, and 9, component B in Fig. 1(a) had been presumed to be identical to component A, except that one was delayed by Δt and phase-biased with respect to the other. (This identity was schematically depicted in Fig. 2 of ref. 9, for example.) This identity is reasonable with regard to the wavelength conversion of clock-like periodical pulses,[1,2] because the carrier density recovers almost linearly in time at a repetition frequency above the carrier cut-off frequency[1] as is schematically depicted in Fig. 2(a). This identity would, however, not be the case in the wavelength conversion of random data pulses where the carrier recovery is accelerated with a strong CW input that is acting as a holding beam;[11] consequently, it should recover exponentially in time after each '1' data pulse (Fig. 2(b)). The exponential recovery of the carrier density should induce an exponential recovery of the nonlinear refractive-index change inside the SOA. If the two-split components are identical with each other and their optical phases recover exponentially (Fig. 3(a)), the optical phase difference between the two components will not stay

*E-mail address: y.ueno@ieee.org

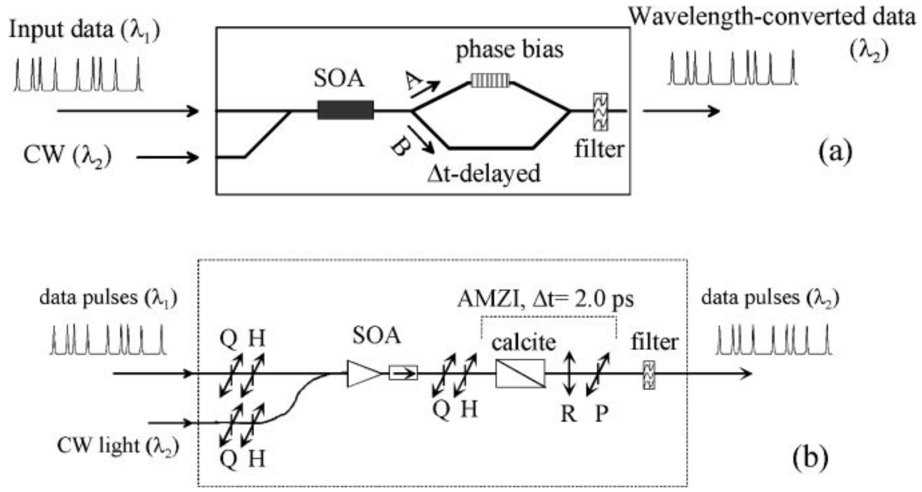

Fig. 1. Delayed-interference signal-wavelength convertor (DISC).[1,9] SOA: semiconductor optical amplifier. Q: quarter-wave plate. H: half-wave plate. P: polarizer. R: optical phase retarder.

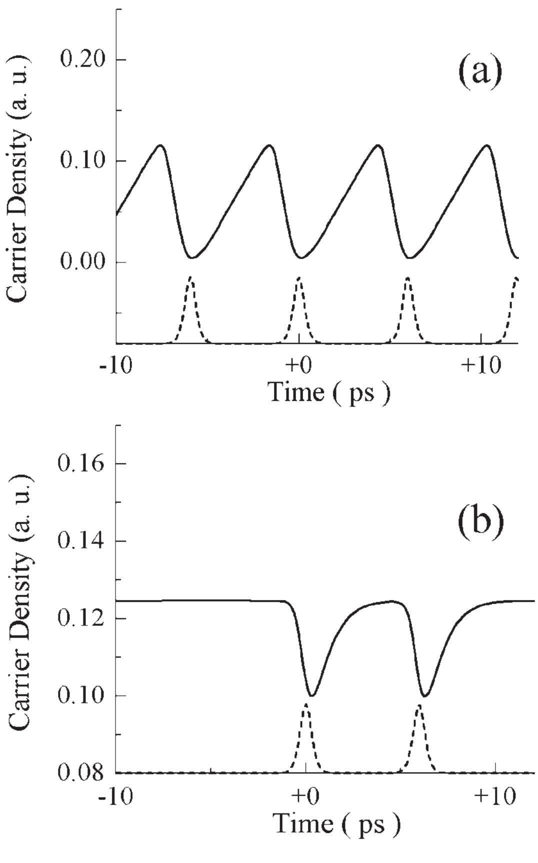

Fig. 2. Carrier-density oscillation inside the DISC. (a) with wavelength-converting clock-like periodical pulses. (b) with wavelength-converting data pulses. Solid curves: carrier-density oscillation. Dashed curves: waveforms of the input pulses to the SOA.

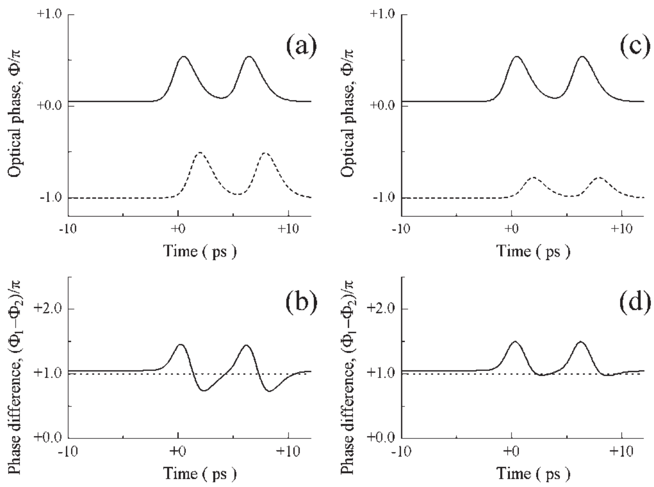

Fig. 3. Optical phases of the co-propagating CW components (when converting random signal pulses). Solid and dashed curves in (a) and (c): optical phases of the non-delayed (A) and delayed (B) CW components in Fig. 1, respectively, before the interference. (b) and (d): phase difference between components A and B. (a) and (b): when the nonlinear phase shifts of the two components are balanced. (c) and (d): when the nonlinear phase shifts of the two components are unbalanced.

at π outside of the gating window (Fig. 3(b)). In such a case, the wavelength-converted data pulses will be accompanied by noisy sub-pulses (Fig. 4(d)).

As long as the time-averaged auto-correlation trace of the 168-Gb/s wavelength-converted signals in the previous experiment was concerned, such noisy sub-pulses were not observed.[5,7] The present authors have therefore speculated that two-split components A and B were not identical in the experiment. Thus, we have searched for a hidden condition that is required for high-quality wavelength conversion.

To search for the additional condition, we theoretically calculated pseudorandom data pulse waveforms at the DISC output while widely varying each operating condition. The conceptual DISC structure in Fig. 1(a) was assumed for simplicity in these searches. The feasibility of our theoretical model, where XPM, XGM, and the pulse gain saturation were taken into account, has been experimentally verified with clock-like periodical input pulses in several ways.[1,7,12] The theoretical equations of the model are briefly described in Appendix. The bitrate, the input pulse width, the delay time Δt, and the pulse shape in this work were assumed to be 168 Gb/s, 1.5 ps, 1.5 ps, and secant-hyperbolic, respectively. The interferometer's phase bias value was optimized for each set of operating conditions. The parameters used to obtain the following results are summarized in Tables I and II.

Table I. Input pulse parameters.

Description	Value
Bitrate	168 Gb/s
Signal pulse width	1.5 ps
Signal pulse energy	3.0 fJ
Signal power	−6.0 dBm
Pseudorandom word length	2^{15}–1
Input CW light power	0 dBm

Table II. DISC's parameters.

Parameter	Description	Value
G_0	Unsaturated gain	28 dB
P_{sat}	Gain saturation energy	180 fJ
$\Delta\Phi_{max}{}^{1,2}$	Phase shift at complete carrier depletion, $\Delta\Phi(\Delta n_c = n_c^0)$	$+3.00\pi$, $+1.35\pi$
$\Delta\Phi_{max}{}^{1}/\Delta\Phi_{max}{}^{2}$	Phase imbalance factor	0.45
τ_c	Carrier lifetime	30 ps
$I_{op}{}^{0}$	Nominal injection current	150 mA
I_{op}	Enhanced current injection	1,000 mA
$I_{op}{}^{enh}$	Injection enhancement factor	6.6
Δt	Delay time for the interference	1.5 ps
$\Delta\Phi_b$	Interferometer phase bias	1.050π

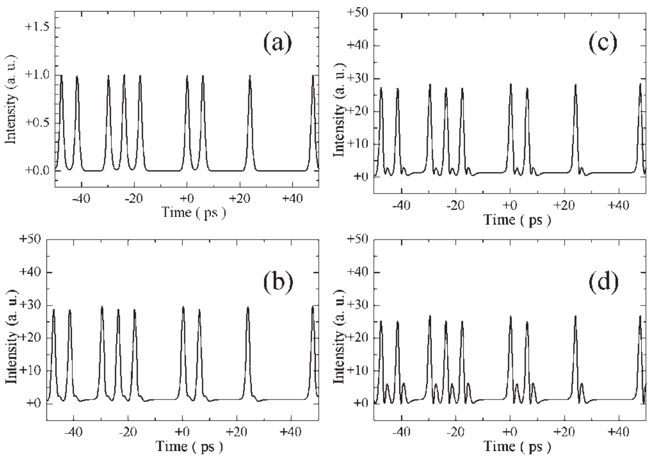

Fig. 4. Calculated input waveform (a) and output waveforms (b)–(d). The ratio of the nonlinear phase shift of the delayed component B to that of the non-delayed component A was set to (b) 0.45, (c) 0.70, and (d) 1.00.

As a result of our numerical searches, we found that the sub-pulses in Fig. 4(d) are almost suppressed only when the magnitude of the nonlinear phase shift for delayed component B is optimized separately from that of non-delayed component A, as shown in Fig. 4. The sub-pulse suppression in the figure occurs because the phase difference between the two components now stays at π outside of the gating window (Fig. 3(d)). It should be noted that the amplitude of the delayed component B was intentionally set equal to that of the non-delayed component A, for realizing the destructive interference outside of the switching window.

Figures 5(a) and 5(b) show the output eye diagrams obtained from the results in Figs. 4(b) and 4(d), respectively. When the imbalance factor between the nonlinear phase shifts of the two-split components was optimized to 0.45 in this example, a clear eye was obtained (Fig. 5(a)). Data-pattern-induced noise was negligibly small. These eye diagrams were drawn by superimposing 1024 consecutive pseudorandom pulse waveforms. The pseudorandom pattern length in the calculation was set to 2^{15}-1 (i.e., much larger than 1024). The magnitude of the nonlinear phase shift for the non-delayed component in the results of Figs. 4 and 5 was set nearly equal (0.23π) to that (0.2π-0.3π) estimated in the 168-Gb/s experiment.[7)]

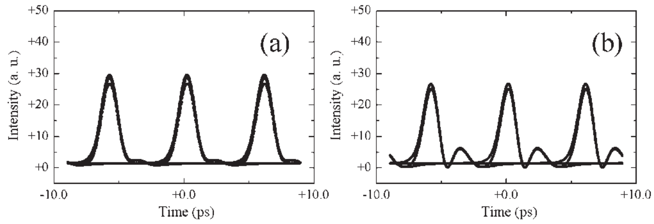

Fig. 5. Calculated eye diagrams of the wavelength-converted pulses with and without the phase balance adjustment. The ratio between the nonlinear phase shifts was set to (a) 0.45 and (b) 1.00, respectively. Each eye diagram was drawn by superimposing 1024 consecutive pseudorandom pulse waveforms.

In conclusion, we have theoretically predicted that an imbalance between the magnitudes of the nonlinear phase shift in two-split interference components is *required* for wavelength conversion of random data pulses. Because the noisy sub-pulses were not observed in the averaged waveforms of the 168-Gb/s converted signal in the previous conversion experiment, we speculate that this requirement was partially fulfilled probably because of the waveplate optimizations in the experiment along with an additional nonlinear effect such as nonlinear polarization rotation[13,14)] in the SOA. We also speculate that this requirement was fulfilled *only partially*, which has caused the significant noise in the demultiplexed-and-sampled 10.5-Gb/s eye diagrams and the power penalty in the previously-reported error-rate measurement. Further designs of the DISC wavelength conversion scheme with taking the new nonlinear phase requirement into account will lead to higher-quality wavelength conversion of such ultrafast optical data signals.

1) Y. Ueno *et al.*: Opt. Lett. **23** (1998) 1846.
2) Y. Ueno *et al.*: Jpn. J. Appl. Phys. **39** (2000) L806.
3) Y. Ueno *et al.*: ECOC 2000, Vol. 1, p. 13.
4) J. Leuthold *et al.*: Electron. Lett. **36** (2000) 1129.
5) S. Nakamura *et al.*: IEEE Photonics Technol. Lett. **13** (2001) 1091.
6) J. Leuthold *et al.*: Opt. Quantum Electron. **33** (2001) 939.
7) Y. Ueno *et al.*: J. Opt. Soc. Am. B **19** (2002) 2573.
8) J. Leuthold *et al.*: Electron. Lett. **38** (2002) 890.
9) Y. Ueno *et al.*: IEEE Photonics Technol. Lett. **10** (1998) 346.
10) K. Tajima: Jpn. J. Appl. Phys., **32** (1993) L1746.
11) R. Manning *et al.*: Opt. Lett. **19** (1994) 889.
12) Y. Ueno *et al.*: IEICE Trans. Electron. **E86-C** (2003) 731.
13) H. Sato *et al.*: IEEE Photonics Technol. Lett. **11** (1999) 970.
14) R. J. Manning *et al.*: Electron. Lett. **37** (2001) 229.

Appendix: Equations and material parameters used in the theoretical model[1,7,12)]

In our theoretical model, the integral of nonlinear change in the refractive index from the input through the output of the SOA is assumed to be proportional to the averaged carrier-density change over the interaction distance, $\{n_c^0 -$

$\overline{n_c(t)}\}$. Consequently, the nonlinear phase shift of the cross-phase-modulated CW light at the SOA output is described as a function of time as,

$$\Phi(t) = k_0 \cdot dn_r/dn_c \cdot \{n_c^0 - \overline{n_c(t)}\} \cdot \Gamma L, \qquad \text{(A·1)}$$

where k_0 is the wave number in vacuum, n_r is the refractive index, and Γ is the optical confinement factor of the propagating optical components within the cross section of the active layer in the SOA. L is the length of the SOA. The equilibrium excess carrier density, ${n_c}^0$, is defined as the excess carrier density at which the SOA does not receive any input light.

The change in the material gain is also assumed to be proportional to the carrier-density change. As a result of this assumption, the SOA's chip gain is expressed as,

$$G(t) \equiv \exp[dg/dn_c \cdot \overline{n_c(t)} \cdot \Gamma L]. \qquad \text{(A·2)}$$

The dynamics of both the nonlinear phase shift and the chip gain are governed by a rate equation for the averaged carrier density, which is assumed to be

$$\frac{d}{dt}\overline{n_c(t)} = \frac{I_{op}}{qV} - \frac{\overline{n_c(t)}}{\tau_c} - \frac{1}{V} \cdot (G\{\overline{n_c(t)}\} - 1) \cdot \frac{|E_{pulse}(t)|^2 + |E_{CW}|^2}{\hbar\omega}, \qquad \text{(A·3)}$$

where I_{op} is the injected current, q is the elementary charge, τ_c is the carrier lifetime, and V is the volume of the current-injected active layer of the SOA. The first, the second, and the third terms in the r.h.s. represent the injection of carriers, the relaxation of carriers, and the stimulated recombination that is induced by input pulses $[E_{pulse}(t)]$ and the co-propagating strong CW light $[E_{CW}]$, respectively.

Finally, the wavelength-converted output pulse waveform is expressed as,

$$E_{OUT}(t) = \frac{1}{2}\Big(\sqrt{G(t)}\exp[i\Phi(t) + \Delta\Phi_b]E_{CW} + \sqrt{G(t-\Delta t)}\exp[i\Phi(t-\Delta t) \times f_{phase}]E_{CW}\Big), \qquad \text{(A·4)}$$

where $\Delta\Phi_b$ is the static phase bias between the two interference components. The first term in the r.h.s. represents the non-delayed interference component A in Fig. 1(a), while the second term represents the delayed interference component B. As a result of our theoretical searches in this work, the phase imbalance factor f_{phase} ($0.45 \leq f_{phase} \leq 1.0$ in Fig. 4) has newly been introduced.